

## Synthesis and properties of stable amorphous hole-transporting molecules for electroluminescent devices

Vinich Promarak,<sup>a,\*</sup> Musubu Ichikawa,<sup>b</sup> Duongratchaneekorn Meunmart,<sup>a</sup> Taweesak Sudyoasuk,<sup>a</sup> Sayant Saengsuwan<sup>a</sup> and Tinnagon Keawin<sup>a</sup>

<sup>a</sup>Department of Chemistry, Faculty of Science, Ubon Ratchathani University, Warinchumrap, Ubon Ratchathani, Thailand

<sup>b</sup>Department of Functional Polymer Science, Shinshu University, Ueda, Nagano 386-8567, Japan

Received 29 August 2006; revised 27 September 2006; accepted 5 October 2006

**Abstract**—New triphenylamine–carbazole end-capped molecules were synthesized by a divergent approach using bromination and Suzuki cross-coupling reactions. All compounds showed an excellent electrochemical reversibility and a good thermal stability. They were fabricated as hole-transporting layers (HTLs) with the device configuration of ITO/HTL/Alq<sub>3</sub>/LiF:Al. A bright green emission from the Alq<sub>3</sub> layer with a maximum luminance of 7500 cd/m<sup>2</sup> was observed at 9.8 V and a low turn-on voltage of 3.4 V. © 2006 Elsevier Ltd. All rights reserved.

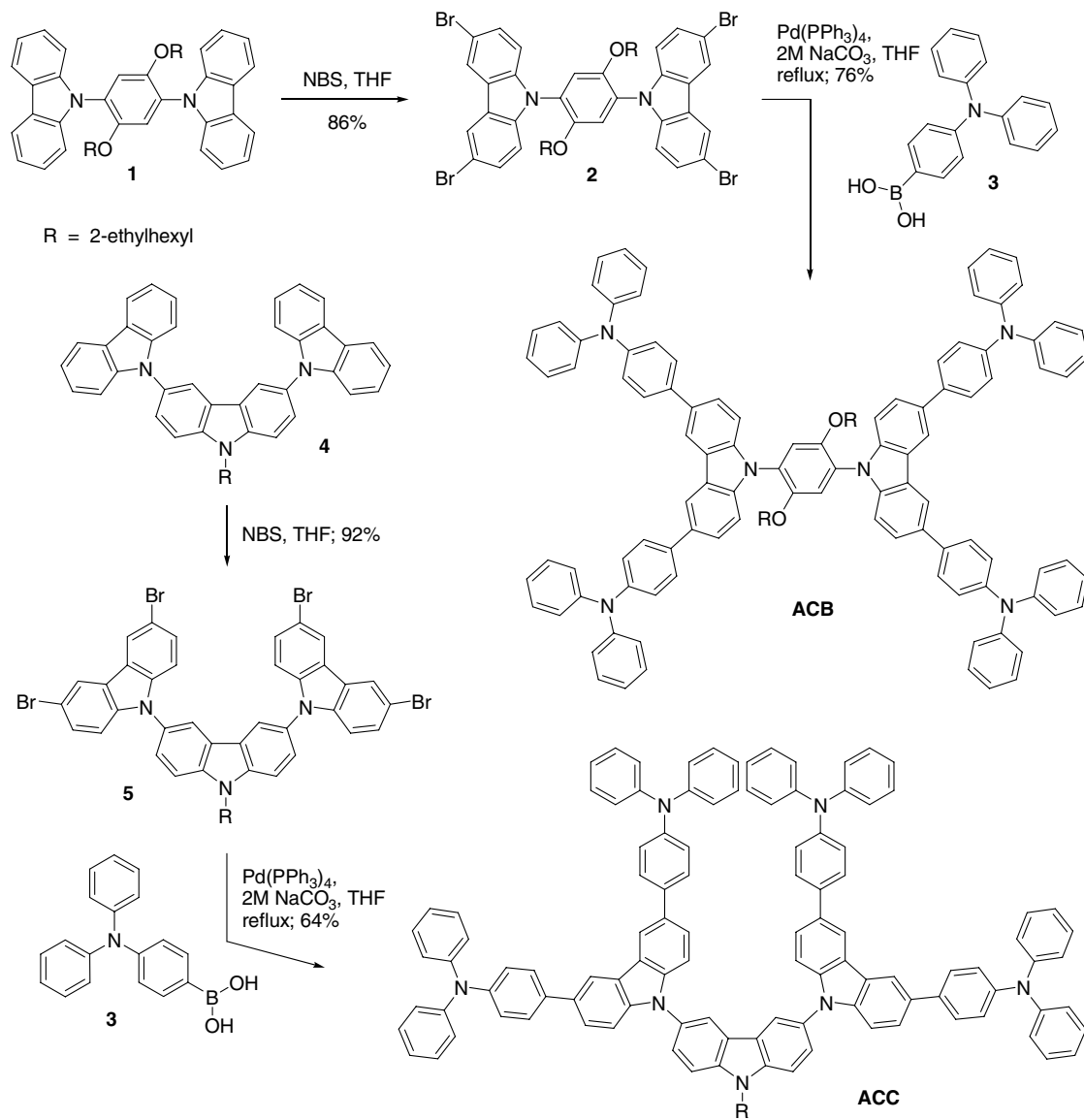
Organic light-emitting diodes (OLEDs) have attracted a great deal of attention because of their potential applications to low-cost, full color flat panel displays.<sup>1</sup> The past decade has seen great progress in both device fabrication techniques and material developments.<sup>2</sup> Tang and VanSlyke have made a key progress in the field by demonstrating that the use of hole transporting layers (HTLs) for hole injection from the anodes into the light-emitting layer (EL) provides significant improvement in the OLED device performance.<sup>3</sup> Since, many new hole-transporting materials have been developed.<sup>4,5</sup> In particular, low-molecular weight amorphous materials have received interest as candidates for HTL materials due to their easy purification by vapor deposition or column chromatographic techniques and uniform thin films can be simply processed by coating techniques. In order to achieve highly efficient and long lifetime devices, an amorphous hole-transporting material (AHTM) with high mobility, high glass transition temperature ( $T_g$ ), a stable amorphous state and a good thin film formation is desirable. Optimization of all these requirements is still a difficult challenge for scientists. So far, many AHTMs with high  $T_g$  values such as carbazole derivatives containing peripheral diarylamine units,<sup>6</sup> dicarbazoyl derivatives featuring peripheral diphenylamine units,<sup>7</sup> and triaryldiamines containing a

spiro(adamantane-2,9-fluorene) core<sup>8</sup> have been reported. More recently, triarylamine–carbazole end-capped oligofluorenes have been prepared using a convergent approach, but their device properties have not been reported.<sup>9</sup> In this letter, we report the synthesis and characterization of the new triphenylamine–carbazole dendrimers, which are conveniently prepared by a divergent approach in two steps. Their hole-transporting properties were investigated by preparing double-layer devices with the light-emitting material, Alq<sub>3</sub>.

The target molecules **ACB** and **ACC** were synthesized as illustrated in **Scheme 1**. Compounds **1** and **4** which have been prepared in our laboratory<sup>10</sup> were first selectively brominated with NBS in THF at room temperature. As a result, only the most nucleophilic 3- and 6-positions of the peripheral carbazoles were substituted to give the corresponding tetrabromine compounds **2** and **5** in good yields.<sup>11</sup> Next, these were coupled with an excess of triphenylamine boronic acid **3** under Suzuki cross-coupling conditions in the presence of Pd(PPh<sub>3</sub>)<sub>4</sub> as a catalyst and an aqueous solution of Na<sub>2</sub>CO<sub>3</sub> as the base in THF at reflux to afford the target compounds **ACB** and **ACC** in 76% and 64% yields, respectively. Both **ACB** and **ACC** were soluble in all common organic solvents and their structures were confirmed by IR, <sup>1</sup>H, <sup>13</sup>C NMR, and HRMS spectrometric methods.<sup>11</sup>

The optical properties of **ACB** and **ACC** were investigated by UV–vis and photoluminescent spectroscopy

\* Corresponding author. Tel.: +66 81 5930005; fax: +66 45 288379; e-mail: [pvinich@sci.ubu.ac.th](mailto:pvinich@sci.ubu.ac.th)



**Scheme 1.** Synthetic routes to the targets **ACB** and **ACC**.

in dilute CH<sub>2</sub>Cl<sub>2</sub> solution (Fig. 1 and Table 1). The absorption spectra of **ACB** and **ACC** were dominated by strong broad absorption peaks at around 336 and 330 nm, respectively, which are derived from the combination of absorption from the triphenylamine–carbazole peripheral units and the conjugated backbone. The spectra were substantially red-shifted (~30 nm) relative to the spectra of compounds **1** and **4**, attributed to the conjugation of the triphenylamine groups with the interior unit leading to a decrease in the energy gap. Moreover, in comparison to the absorption maxima of the triphenylamine–carbazole unit,<sup>9</sup> the absorption maxima of **ACB** and **ACC** were about 6–12 nm red-shifted suggesting  $\pi$ -conjugation between the triphenylamine–carbazole and the aromatic cores through the electron lone pair on the nitrogen atom of the carbazole and that the  $\pi$ -electrons were delocalized over the entire conjugated backbone. The UV–vis spectra of **ACB** and **ACC** exhibited the onset of absorptions ( $\lambda_{\text{onset}}$ ) at 375 and 379 nm corresponding to energy band gaps of 3.31

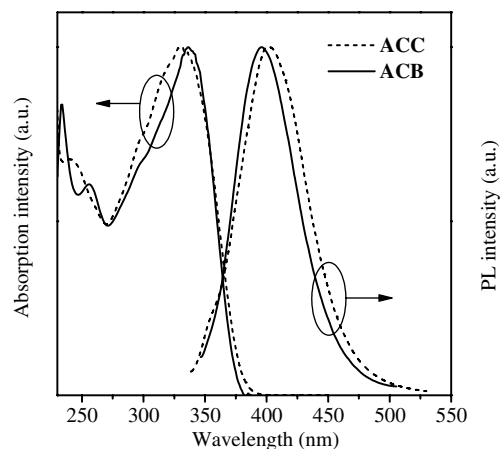


**Figure 1.** Optical properties of compounds **ACB** and **ACC** in CH<sub>2</sub>Cl<sub>2</sub> solution.

and 3.27 eV, respectively. The photoluminescent spectra of **ACB** and **ACC**, excited at 325 nm, were located in the

**Table 1.** Summary of the physical measurements of **ACB** and **ACC**

Comp	$\lambda_{\max}^{\text{abs}}$ <sup>a</sup> /nm (log $\epsilon$ /dm <sup>3</sup> mol <sup>-1</sup> cm <sup>-1</sup> )	$\lambda_{\max}^{\text{em}}$ <sup>b</sup> /nm	$T_g$ <sup>c</sup> /°C	$T_{5d}$ <sup>d</sup> /°C	$E_{1/2}/V(\Delta E^e/\text{mV})$	$E_g$ <sup>f</sup> /eV	HOMO <sup>g</sup> /eV	LUMO <sup>h</sup> /eV
<b>ACB</b>	336(5.33)	393	121	415	1.04(180), 1.26(240)	3.31	5.37	2.06
<b>ACC</b>	330(5.18)	401	185	415	1.04(180), 1.26(220)	3.27	5.37	2.10

<sup>a</sup> Measured in a dilute CH<sub>2</sub>Cl<sub>2</sub> solution.

<sup>b</sup> Excited at 325 nm.

<sup>c</sup> Obtained from DSC measurements on the second heating cycle with a heating rate of 10 °C/min under N<sub>2</sub>.

<sup>d</sup> Obtained from TGA measurements with a heating rate of 10 °C/min under N<sub>2</sub>.

<sup>e</sup> Measured using a platinum disk as a working electrode, a platinum rod as a counter electrode, and SCE as a reference electrode in CH<sub>2</sub>Cl<sub>2</sub> containing 0.1 M *n*-Bu<sub>4</sub>NClO<sub>4</sub> as a supporting electrolyte at a scan rate of 50 mV/s under an argon atmosphere.

<sup>f</sup> Estimated from the onset of absorption ( $E_g = 1240/\lambda_{\text{onset}}$  eV).

<sup>g</sup> Calculated by the empirical equation: HOMO = (4.44 +  $E_{\text{onset}}$ ).<sup>12</sup>

<sup>h</sup> Calculated from LUMO = HOMO –  $E_g$ .

bluish-purple region with emission peaks at 393 and 401 nm, respectively.

The thermal properties of **ACB** and **ACC** were measured using differential scanning calorimetry (DSC) and thermogravimetric analysis (TGA) under N<sub>2</sub> (Table 1). TGA analysis revealed that both compounds were thermally stable with 5% weight loss temperatures ( $T_{5d}$ ) being observed at 415 °C. DSC measurements after the samples of **ACB** and **ACC**, prepared by crystallization from a mixture of dichloromethane and methanol, had first been heated to 320 °C showed sharp endothermic peaks due to melting ( $T_m$ ) at 183 and 239 °C, respectively. These were not detected during the second heating scan and only an endothermic baseline shift due to glass transitions ( $T_g$ ) were observed at 121 and 185 °C, respectively. On further heating, no peaks due to crystallization and melting appeared. The ability of **ACB** and **ACC** to form a molecular glass and the possibility of preparing thin films from **ACB** and **ACC** both by evaporation and by solution casting are highly desirable for applications in OLEDs.

The redox properties and HOMO and LUMO energy levels of compounds **ACB** and **ACC** were investigated using cyclic voltammetry (CV). The results are summarized in Table 1. Both **ACB** and **ACC** showed two chemically reversible oxidation processes. Their first and second oxidation processes were observed at potentials of 1.04 and 1.26 V, respectively, separated by 220 mV. The first oxidation can be assigned to the simultaneous multielectron oxidation process of the peripheral triphenylamine group, while the second oxidation corresponds to the removal of electrons from the interior moieties. Moreover, their CV curves also exhibited the same onset oxidation potentials ( $E_{\text{onset}}$ ), which were estimated from the first anodic oxidation wave to be 0.93 V. As a result, HOMO levels were calculated to be 5.37 eV and the LUMO levels of **ACB** and **ACC** were calculated to be 2.06 and 2.10 eV, respectively, by subtracting the energy band gaps (3.31 and 3.27 eV) from the HOMO energy level. The high-lying HOMO energy levels and reversible electrochemical oxidations of **ACB** and **ACC** suggest that both compounds have potential for hole injection and transport in OLED.<sup>13</sup>

In order to investigate their hole-transporting properties, the double-layer OLED devices of ITO/HTL

(50 nm)/Alq<sub>3</sub> (200 nm)/LiF (0.5 nm):Al (200 nm) were fabricated using **ACB** or **ACC** as the hole-transporting layer (HTL), Alq<sub>3</sub> as the light-emitting and electron-transporting layers, indium tin oxide (ITO) as the anode and LiF:Al as the cathode. When a bias potential was applied to the electrodes, the ITO/**ACB**/Alq<sub>3</sub>/LiF:Al and ITO/**ACC**/Alq<sub>3</sub>/LiF:Al devices emitted bright green luminescence with emission maxima of 522 and 520 nm, respectively. The EL spectra were in agreement with the PL spectrum of Alq<sub>3</sub> and also other reported EL spectra of Alq<sub>3</sub>. This indicates that the ELs from the devices consisting of Alq<sub>3</sub> and either **ACB** or **ACC** show no emission at the longer wavelength from the exciplex species. Such interference is often observed in devices using planar molecules.<sup>14</sup> In these cases, the exciplex formation is prevented by the bulky triphenylamine-carbazole dendron at both ends of the molecules. Moreover, this also suggests that both **ACB** and **ACC** are only hole-transporting materials and the electron-hole recombination takes place at the Alq<sub>3</sub> emitting layer. The voltage-luminance and voltage-current density characteristics of the devices are shown in Figure 2. The device using **ACC** as a HTL has much better performance in terms of brightness, current and turn-on voltage than that using **ACB**. In the case of the ITO/**ACC**/Alq<sub>3</sub>/LiF:Al device, the maximum luminance was about 7500 cd/m<sup>2</sup> at 9.8 V with a turn-on voltage of 3.4 V. The

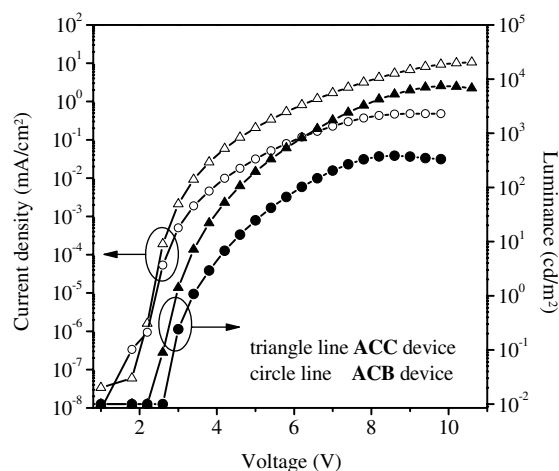


**Figure 2.** Voltage vs current density and luminance characteristics of **ACB** and **ACC** devices.

ITO/ACB/Alq<sub>3</sub>/LiF:Al device showed a maximum luminance at 390 cd/m<sup>2</sup> at 8.6 V with a turn-on voltage of 4.2 V.

In conclusion, we have successfully synthesized novel amorphous hole-transporting molecules, **ACB** and **ACC** using a divergent route involving bromination and Suzuki cross-coupling reactions. Both compounds exhibited an excellent electrochemical reversibility and a high thermal stability. The double-layer OLED device containing **ACC** as the HTL showed the best performance with a bright green emission of 7500 cd/m<sup>2</sup> at 9.8 V and a low turn-on voltage of 3.4 V. The use of triphenylamine-carbazole end-caps might be an effective way to prepare amorphous molecules for OLEDs by forming dendritic structures with other fluorescent or nonfluorescent core units.

### Acknowledgments

This work is supported by the National Nanotechnology Center of Thailand (Grant Code: NN-B-22-e1-25-47-07). We thank the Chulabhorn Research Institute (CRI) for the HRMS measurements.

### References and notes

- Hide, F.; Diaz-Garcia, M. A.; Schartz, B. J.; Heeger, A. J. *Acc. Chem. Res.* **1997**, *30*, 430–436.
- Forrest, S. R. *Org. Electron.* **2003**, *4*, 45–48.
- Tang, C. W.; VanSlyke, S. A. *Appl. Phys. Lett.* **1987**, *51*, 913–915.
- Shirota, Y. *J. Mater. Chem.* **2000**, *10*, 1–26.
- Lu, J.; Tao, Y.; D'iorio, M.; Li, Y.; Ding, J.; Day, M. *Macromolecules* **2004**, *37*, 2442–2449.
- Thomas, K. R. J.; Lin, J. T.; Tao, Y.-T.; Ko, C.-W. *J. Am. Chem. Soc.* **2001**, *123*, 9404–9411.
- Kundu, P.; Thomas, K. R. J.; Lin, J. T.; Tao, Y.-T.; Chein, C.-H. *Adv. Func. Mater.* **2003**, *13*, 445–452.
- Chen, C.-H.; Shen, W.-J.; Jakka, K.; Shu, C.-F. *Synth. Met.* **2004**, *143*, 215–220.
- Li, Z. H.; Wong, M. S. *Org. Lett.* **2006**, *8*, 1499–1502.
- Laijarernkit, N.; Werawong, P.; Palasak, W. B.Sc. Thesis, Ubon Ratchathani University, 2003.
- Physical data for **2**: mp 204 °C; IR (KBr) 2923, 1518, 1467, 1281, 1215, 1020, and 801 cm<sup>-1</sup>; <sup>1</sup>H NMR (300 MHz, CDCl<sub>3</sub>) δ 0.57 (6H, t, *J* = 7.5 Hz), 0.70 (6H, t, *J* = 7.2 Hz), 0.84–0.97 (16H, m), 1.25–1.29 (2H, m), 3.66 (4H, dd, *J* = 2.7 Hz, *J* = 2.7 Hz), 7.18 (4H, d, *J* = 8.4 Hz), 7.30 (2H, s, *J* = 3.6 Hz), 7.55 (4H, dd, *J* = 7.2 Hz, *J* = 1.5 Hz), 8.24 (4 H, d, *J* = 1.8 Hz); <sup>13</sup>C NMR (75 MHz, CDCl<sub>3</sub>) 10.81, 13.86, 22.73, 23.38, 28.75, 30.20, 39.13, 50.88, 72.18, 112.02, 113.09, 115.44, 123.14, 124.02, 126.10, 129.24, 140.23, and 149.69; HRMS-ESI *m/z*: [MH<sup>+</sup>] calcd for C<sub>46</sub>H<sub>49</sub>Br<sub>4</sub>N<sub>2</sub>O<sub>2</sub>, 977.0522. Found: 977.0545. **ACB**: mp >280 °C; IR (KBr) 2915, 1590, 1480, 1277, 1229, 1026, and 805 cm<sup>-1</sup>; <sup>1</sup>H NMR (300 MHz, CDCl<sub>3</sub>) δ 0.59 (6H, t, *J* = 7.5 Hz), 0.66 (6H, t, *J* = 6.9 Hz), 0.92–1.04 (16H, m), 1.28–1.33 (2H, m), 3.72 (4H, d, *J* = 5.4 Hz), 7.06 (8H, t, *J* = 6.9 Hz), 7.18–7.25 (22H, m), 7.28–7.34 (18H, m), 7.41 (6H, d, *J* = 9.9 Hz), 7.65 (8H, d, *J* = 8.4 Hz), 7.70 (4H, d, *J* = 8.4 Hz), and 8.41 (4H, s); <sup>13</sup>C NMR (75 Hz, CDCl<sub>3</sub>) δ 10.84, 13.91, 22.77, 23.41, 28.79, 30.22, 39.19, 72.31, 110.7, 115.86, 118.30, 122.72, 124.09, 124.23, 124.46, 125.10, 126.68, 127.94, 129.25, 132.98, 136.43, 141.06, 146.52, 147.86, and 149.90; HRMS-ESI *m/z*: [MH<sup>+</sup>] calcd for C<sub>118</sub>H<sub>105</sub>N<sub>6</sub>O<sub>2</sub>, 1637.8294. Found: 1637.8392. Compound **5**: mp 220 °C; IR (KBr) 2927, 1492, 1279, 1231, 1021, and 801 cm<sup>-1</sup>; <sup>1</sup>H NMR (300 Hz, CDCl<sub>3</sub>) δ 0.95 (3H, t, *J* = 6.9 Hz), 1.06 (3H, t, *J* = 7.5 Hz), 1.34–1.59 (8H, m), 2.19–2.25 (1H, m), 4.37 (2H, d, *J* = 6.3 Hz), 7.25 (4H, d, *J* = 8.7 Hz), 7.49 (4H, dd, *J* = 6.9 Hz, *J* = 1.8 Hz), 7.59 (2H, dd, *J* = 1.8 Hz, *J* = 8.4 Hz), 7.67 (2H, d, *J* = 8.7 Hz), 8.17 (2H, d, *J* = 1.2 Hz), 8.23 (4H, d, *J* = 1.8 Hz); <sup>13</sup>C NMR (75 MHz, CDCl<sub>3</sub>) 11.00, 14.04, 23.10, 24.56, 28.87, 31.10, 39.69, 48.11, 110.71, 111.48, 119.64, 123.21, 123.31, 123.73, 125.74, 128.49, 129.33, 140.82, and 140.96; HRMS-ESI *m/z*: [MH<sup>+</sup>] calcd for C<sub>44</sub>H<sub>36</sub>Br<sub>4</sub>N<sub>3</sub>, 921.9637. Found: 921.9665. **ACC**: mp >280 °C; IR (KBr) 2922, 1590, 1487, 1277, 1019, and 809 cm<sup>-1</sup>; <sup>1</sup>H NMR (300 MHz, CDCl<sub>3</sub>) δ 0.96 (3 H, t, *J* = 6.9 Hz), 1.08 (3H, t, *J* = 7.2 Hz), 1.38–1.49 (8H, m), 2.27 (1H, s), 4.39 (2H, d, *J* = 6.6 Hz), 7.04 (8H, t, *J* = 7.2 Hz), 7.15–7.21 (24H, m), 7.26–7.31 (16H, m), 7.45 (4H, d, *J* = 8.4 Hz), 7.61–7.67 (12 H, m), 7.72 (4H, s), 8.31 (2H, s), and 8.40 (4H, s); <sup>13</sup>C NMR (75 Hz, CDCl<sub>3</sub>) δ 11.04, 14.09, 23.14, 24.60, 28.91, 31.14, 39.72, 110.11, 110.47, 118.39, 119.60, 122.69, 123.41, 132.82, 124.19, 124.45, 125.25, 125.78, 127.93, 129.23, 132.87, 136.36, 140.74, 141.55, 146.48, and 147.84; HRMS-ESI *m/z*: [MH<sup>+</sup>] calcd for C<sub>116</sub>H<sub>92</sub>N<sub>7</sub>, 1582.7409. Found: 1582.7351.
- Meng, H.; Zheng, J.; Lovinger, A. J.; Wang, B.-C.; Van Patten, P. G.; Bao, Z. *Chem. Mater.* **2003**, *15*, 1778–1787.
- Chiang, C.-L.; Shu, C.-F. *Chem. Mater.* **2002**, *14*, 682–687.
- Kim, D. Y.; Cho, H. N.; Kim, C. Y. *Prog. Polym. Sci.* **2000**, *25*, 1089–1193.